© 2019. Published by The Company of Biologists Ltd | Journal of Experimental Biology (2019) 222, jeb198705. doi:10.1242/jeb.198705

RESEARCH ARTICLE

High-speed locomotion in the Saharan silver ant, *Cataglyphis bombycina*

Sarah Elisabeth Pfeffer[1,*,‡], Verena Luisa Wahl[1,*], Matthias Wittlinger[1,2,‡] and Harald Wolf[1,‡]

ABSTRACT

The diurnal thermophilic Saharan silver ant, *Cataglyphis bombycina*, is the fastest of the North African *Cataglyphis* desert ant species. These highly mobile ants endure the extreme temperatures of their sand dune environment with outstanding behavioural, physiological and morphological adaptations. Surprisingly, *C. bombycina* has comparatively shorter legs than its well-studied sister species *Cataglyphis fortis* from salt pan habitats. This holds despite the somewhat hotter surface temperatures and the more yielding sand substrate. Here, we report that *C. bombycina* employs a different strategy in reaching high running speeds, outperforming the fastest known runs of the longer-legged *C. fortis* ants. Video analysis across a broad range of locomotor speeds revealed several differences to *C. fortis*. Shorter leg lengths are compensated for by high stride frequencies, ranging beyond 40 Hz. This is mainly achieved by a combination of short stance phases (down to 7 ms) and fast leg swing movements (up to 1400 mm s^{-1}). The legs of one tripod group exhibit almost perfect synchrony in the timings of their lift-offs and touch-downs, and good tripod coordination is present over the entire walking speed range (tripod coordination strength values around 0.8). This near synchrony in leg movement may facilitate locomotion across the yielding sand dune substrate.

KEY WORDS: Stride frequency, High walking speed, Insect, Inter-leg coordination, Aerial phases

INTRODUCTION

Cataglyphis bombycina, better known as the silver ant of the Saharan desert, the Sinai and the deserts of the Arabian Peninsula, occupies the niche of a thermophilic scavenger. This implies foraging activity during the midday sun, when most other desert ants, and indeed desert animals, stop foraging, and preying on the carcasses of arthropods that have succumbed to heat stress. Because of the high midday temperatures, arthropod carcasses accumulate, although at low densities, while predators and competitors have retreated into their burrows (Wehner and Wehner, 2011; Wehner et al., 1992; Wehner, 1987).

To exploit this foraging niche, silver ants need to withstand the extremely hot and dry desert environment. During the hottest hours of the day, the surface temperature of the Saharan sand may easily exceed 60°C (Wehner et al., 1992) and desiccation stress reaches its maximum with very high water vapour saturation deficits (Lighton and Wehner, 1993). Food density is low and long distances may have to be covered during foraging, with shady resting places absent or far apart because of sparse vegetation and mostly blue sky. Moreover, the fluid granular sand medium may impede locomotion and demands considerable energy to cross. To survive such harsh desert conditions, silver ants have evolved a suite of (i) morphological, (ii) physiological and (iii) behavioural traits, as discussed below.

Morphologically, *C. bombycina* is well adapted through a number of features characteristic of the genus *Cataglyphis*. These include special epicuticular hydrocarbons, a favourable volume-to-surface relationship (at least for an insect), a slender alitrunk, powerful muscles and long legs (relative to other ants of more temperate climates) (Sommer and Wehner, 2012; Wehner and Wehner, 2011; Lenoir et al., 2009). Another feature, producing *C. bombycina*'s typical silvery appearance, is triangularly shaped hairs with thermoregulatory effects (Shi et al., 2015; Willot et al., 2016).

Physiologically, the silver ants are adapted to their hot environment through a discontinuous ventilation cycle that reduces respiratory water loss (Lighton and Wehner, 1993; Sommer and Wehner, 2012) and through special properties of heat-shock protein synthesis. It seems that these proteins accumulate prior to heat exposure, enabling *C. bombycina* to tolerate a critical thermal maximum of a body temperature of 53.6±0.8°C (Gehring and Wehner, 1995).

Behaviourally, the ants take advantage of thermal refuges like elevated pebbles or grass blades where available (Wehner and Wehner, 2011) (Fig. 1A). Foraging under just-sublethal heat conditions requires minimization of outdoor activities and a return to the moderate underground temperatures inside the nest to discharge excess heat regularly. Delays in homing may have serious consequences, making an excellent navigation ability and fast and efficient locomotion for straight and rapid homing important survival skills.

In the present study, we examined the silver ants' walking behaviour and walking kinematics across a large speed range to understand how this species achieves its remarkably high walking speeds, particularly in comparison to the longer-legged but slower *C. fortis*. *Cataglyphis fortis* is a thermophilic scavenger (Wehner, 2016), much like *C. bombycina*, although it lives in North African salt pan habitats that typically exhibit baked salty clay substrates in the summer months, as opposed to the sand dune habitat of *C. bombycina*. Are there different strategies in desert ants, and perhaps in animals more generally, to achieve high running speeds?

We expanded the range of recorded walking speeds in *C. bombycina* beyond the known limits (Wehner, 1983; Zollikofer, 1994), to more than 800 mm s^{-1}, and assessed the contribution of different spatial and temporal walking parameters to achieve such speeds and examined in detail gait and leg coordination patterns to gain a deeper understanding of the silver ant's walking behaviour. *Cataglyphis bombycina* combines high stride frequencies, short stance phases and fast swing movements to

[1]Institute of Neurobiology, Ulm University, Albert-Einstein-Allee 11, 89081 Ulm, Germany. [2]Institute of Biology I, University of Freiburg, Hauptstrasse 1, 79104 Freiburg, Germany.
*These authors contributed equally to this work

‡Authors for correspondence (sarah.pfeffer@alumni.uni-ulm.de; matthias.wittlinger@biologie.uni-freiburg.de; harald.wolf@uni-ulm.de)

S.E.P., 0000-0003-1470-5055; V.L.W., 0000-0002-6416-1829

Received 21 December 2018; Accepted 29 August 2019

Journal of Experimental Biology (2019) 222, jeb198705. doi:10.1242/jeb.198705

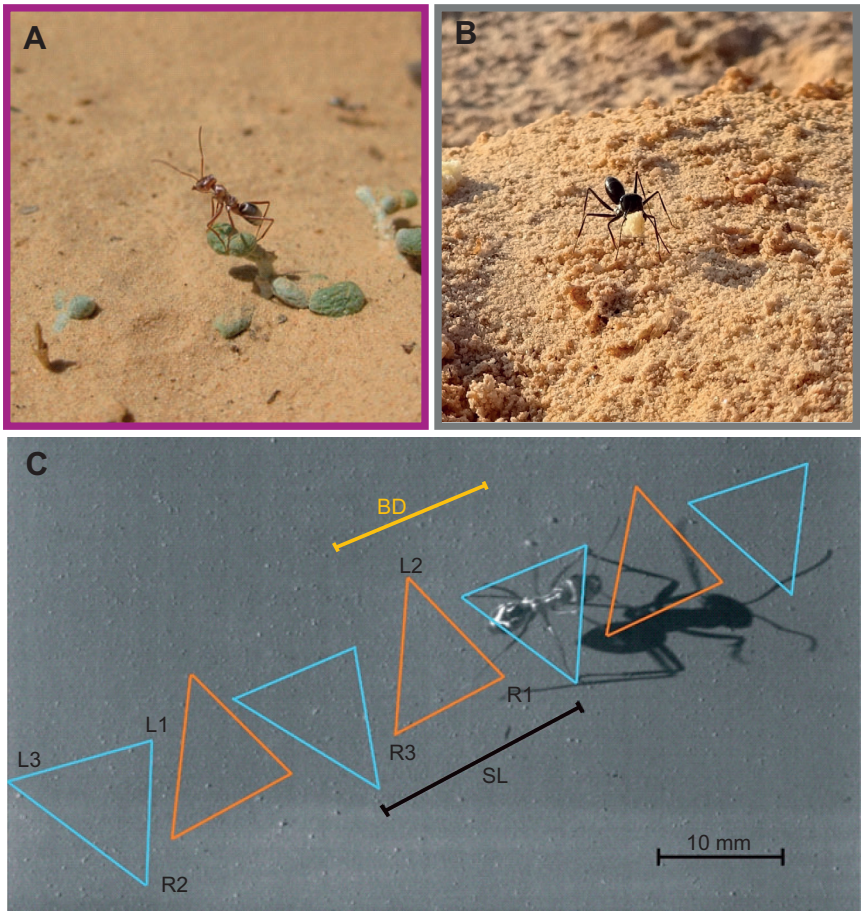

Fig. 1. Study species and high-speed video recording. (A) *Cataglyphis bombycina* in the sand dune habitat of the Saharan desert near Douz, Tunisia. The ant is shown in typical cooling posture on an elevated structure – here, a small succulent plant. The violet frame marks data obtained in *C. bombycina* in subsequent figures. (B) *Cataglyphis fortis* in a salt pan near Menzel Chaker, Tunisia. The homing forager is carrying a food crumb in its mandibles. The grey frame marks data obtained in *C. fortis* in subsequent figures. (C) Tripod gait in *C. bombycina*. A frame from a high-speed video showing an ant during walking at a speed of v=561.4 mm s^{-1}. Several consecutive step cycles were recorded for each leg in the corresponding video sequence (sampling rate 500 Hz). Tripods formed by the left front (L1), hind (L3) and right middle (R2) legs are in blue; tripods formed by the opposite set of legs (R1, L2, R3) are in orange. Stride length (SL) is indicated for the right middle leg, as determined by the distance between two successive footfalls. Stride amplitude can be estimated by subtracting body displacement (BD) from stride length (SL) for the respective swing phase (stride amplitude=SL−BD).

achieve high running speeds, together with the high synchrony of the legs in a tripod.

MATERIALS AND METHODS

Experimental sites and animals

To analyse the characteristics of silver ant (*Cataglyphis bombycina* Roger 1859) locomotion, we compared its morphometry and walking behaviour with that of another desert ant species, *Cataglyphis fortis* (Forel 1902). For morphometric measurements, both ant species were obtained from colonies in their natural habitats. Walking behaviour of *C. bombycina* (Fig. 1C) was recorded near Douz, Tunisia (33.44°N, 9.04°S), and at Ulm University, Germany (48.42°N, 9.95°S), under laboratory conditions. Note that, although walking speeds tended to be higher in the Tunisian desert than under laboratory conditions in Germany, the two datasets overlap and merge smoothly regarding all recorded parameters. All data (n=177 runs) were obtained during the summer months of 2015 and 2016. For comparative purposes, the same procedures were followed for *C. fortis* (n=305 runs) (Fig. 1B). Parts of the latter dataset and corresponding analyses have been published previously (Wahl et al., 2015). The experiments were conducted in compliance with current laws, regulations an ethical guidelines of the University of Ulm and of the country where they were performed.

Morphometric analyses

Lengths of the alitrunk (fused thorax and first abdominal segment, or propodeum) and leg pairs in *C. bombycina* (n=87) and *C. fortis* (n=100) were obtained for morphometric comparison (see Fig. 2). All measurements in *C. bombycina* were performed under a dissection microscope (Stemi SV 6, Zeiss Microskopy GmbH, Jena, Germany) with a measurement eyepiece calibrated with a stage micrometre. All six legs were severed in the coxa–thorax joints before measurement. Lengths of femur, tibia and basitarsus were

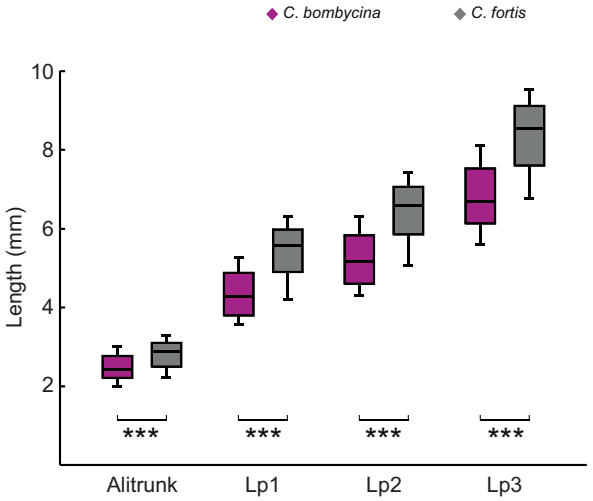

Fig. 2. Morphometric comparison of *C. bombycina* and *C. fortis* alitrunk and leg pair (Lp) lengths. *Cataglyphis bombycina* is significantly smaller than *C. fortis* with respect to mean alitrunk length (11% smaller; *t*-test, ***P<0.001) and mean leg length (first leg pair, 19% shorter, *t*-test, ***P<0.001; second leg pair, 18% shorter, *U*-test, ***P<0.001; third leg pair, 18% shorter, *U*-test, ***P<0.001). Morphometry data of *C. fortis* were kindly provided by S. Sommer and R. Wehner.

Journal of Experimental Biology (2019) 222, jeb198705. doi:10.1242/jeb.198705

determined for front, middle and hind legs. The respective leg lengths were taken as the sum of femur, tibia and basitarsus measurements (e.g. fig. 4 in Zollikofer, 1988; see also Sommer and Wehner, 2012). Alitrunk length was used to characterize body size (see fig. 11 in Agosti, 1990). Most morphological data for *C. fortis* were kindly provided by S. Sommer and R. Wehner.

High-speed videography and experimental procedures

High-speed video equipment (Mikroton MotionBlitz Mini1 high-speed camera, Mikroton, Unterschleissheim, Germany) allowed sampling rates of 500–1000 images s^{-1}. Example videos are available from ResearchGate (doi:10.13140/RG.2.2.21093.45282 and doi:10.13140/RG.2.2.12704.84488) and an extracted single image for each video is shown in the supplementary information (Fig. S2A,B). The ants walked through a linear aluminium channel with a width of 7 cm and a wall height of 7 cm. The floor was coated with fine sand (0.1–0.4 mm particle size) to provide a slip-free substrate for normal walking behaviour. Channel walls were painted with matt grey varnish to avoid distracting reflections. Video recordings were made by mounting the camera above the channel, providing a top view of the walking animals (see Fig. 1C). The highest walking speeds were recorded around noon (11:00 h to 15:00 h) in Douz, Tunisia, with air temperatures of around 45°C. In the laboratory, ants were filmed at different controlled room temperatures (10–30°C) to assess the complete speed range down to 57 mm s^{-1}. For indoor illumination, fibre optic cold light sources (Schott KL 1500LCD, 150 W, Schott AG, Mainz, Germany) were used, while outdoor conditions in Tunisia provided sufficient light for video recordings.

For discrimination, ants were marked individually with car paint (Motip Lackstift Acryl, MOTIP DUPLI GmbH, Haßmersheim, Germany). Ants were usually recorded up to 5 times at different temperatures in order to obtain different walking speeds. Only straight and linear running trajectories with regular stride patterns were used for analyses. That is, walking sequences with abrupt stops, decelerations or accelerations, or curve walking were disregarded. Further, each evaluated recording had to consist of at least three complete step cycles per leg. A piece of millimetre grid paper was used for calibration before a set of videos was recorded. All measurements were digitized with ImageJ (National Institutes of Health, Bethesda, MD, USA) in a frame-by-frame video analysis.

High-speed video analysis and data evaluation

Footfall geometry and centre of mass

To quantify footfall geometry, we measured the *x* and *y* coordinates of tarsal touch-down (just after the end of a swing phase; AEP, anterior extreme position) and tarsal lift-off (just before the start of a swing phase; PEP, posterior extreme position) for each leg with respect to the petiole (Fig. 3A; cf. Seidl and Wehner, 2008; Mendes et al., 2013). The petiole can be regarded as the centre of mass (COM) of an ant (see Reinhardt and Blickhan, 2014). The footprint positions relative to the petiole were normalized to body size; that is, alitrunk

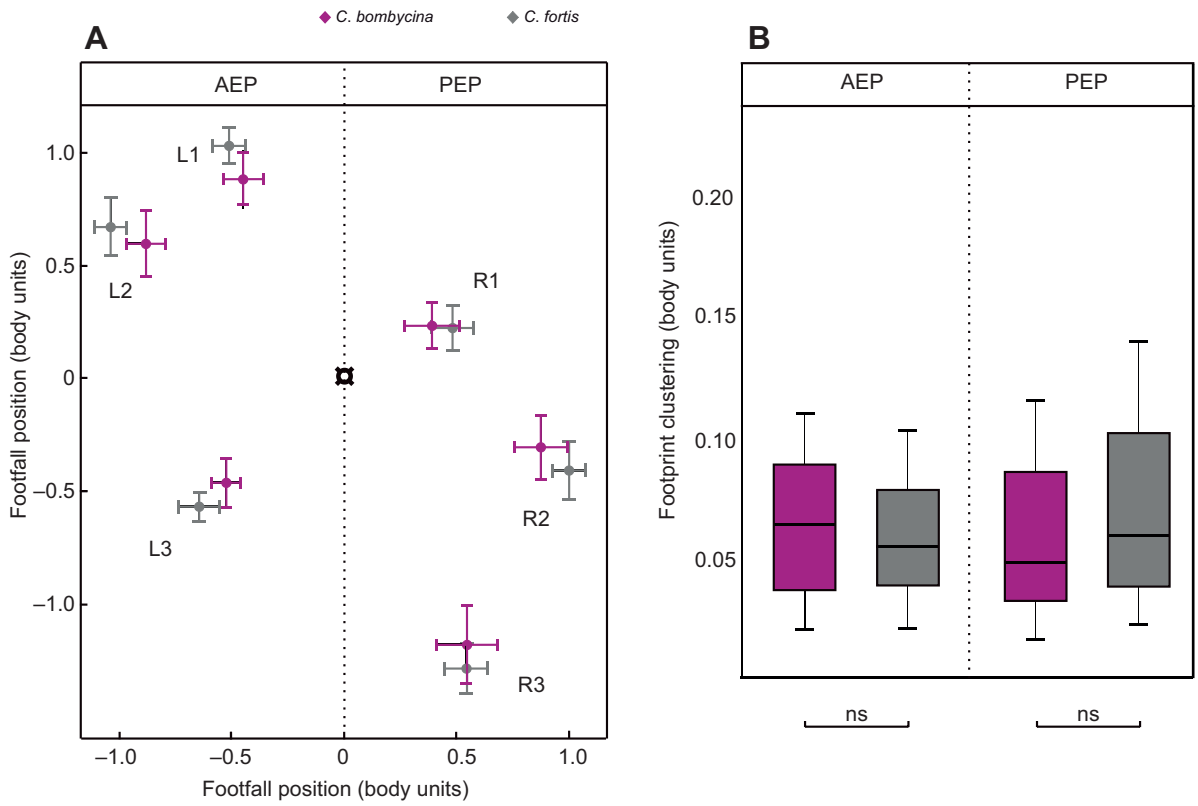

Fig. 3. Footfall geometry. (A) Average footfall positions of the six legs with respect to the petiole [origin of the plot (0/0)]; *x*- and *y*-axes were normalized to the body size of the animals (alitrunk length). For each footfall position, 10 videos with three step cycles each were evaluated, with walking speeds of 490–600 mm s^{-1} for *C. bombycina* and 490–580 mm s^{-1} for *C. fortis*. Anterior extreme positions (AEP) are shown for the left body side (L1, left front leg; L2, left middle leg; L3, left hind leg); posterior extreme positions (PEP) are shown for the right body side (R1, right front leg; R2, right middle leg, R3 right hind leg). (B) The spread of footprints was quantified by calculating standard deviations the of footprint clusters shown in A. Footprint positions show similar spreads in *C. bombycina* and *C. fortis* [Levene's-test, *F*–value AEP=1.3<1.5 (critical value) and *F*-value PEP=1.4<1.5 (critical value)].

length. Standard deviations of footfall positions were used to quantify the spread of footprint positions (footprint clustering in Fig. 3B). Tracks of leg movements and footfall geometry measurements were performed in ImageJ (National Institutes of Health). Movement of the COM was tracked to analyse its horizontal velocity and acceleration (see Figs S4 and S5). Forward velocity (walking speed along the longitudinal axis) was calculated by measuring the distance between the petiole images in two consecutive video frames, and dividing that distance by 1 ms, the frame rate. Forward acceleration is the respective change of forward speed within a 1 ms time interval (see Figs S4 and S5A,B). To determine lateral velocity (along the transverse axis, perpendicular to longitudinal movement), a regression line was first calculated, running through the petiole images in five consecutive video frames. The deviation of the petiole from this regression line was measured in the middle frame. This was done for all video frames (except the initial and final two frames, which did not allow calculation of a regression line). The differences in the lateral deviations in consecutive frames were used to calculate lateral velocity. Lateral acceleration is the respective change of lateral velocity in a 1 ms time interval (see Figs S4 and S5C).

Walking parameters

Different walking parameters were analysed to obtain an overview of the silver ant's locomotor behaviour. We covered a range of 15-fold increase in walking speed, from about 57 to 855 mm s^{-1}, to provide a basis for comprehensive analysis. For all evaluated recordings, the mean walking speed was calculated as the distance covered from the start of the first step cycle to the end of the last step cycle in a given video sequence, divided by the time needed to cover that distance. Further, the timing of each lift-off and touch-down event of the six tarsal tips was measured. The swing phase was considered to be the time between tarsal touch-down and lift-off; that is, the time of tarsal tip movement. A leg was defined to be in stance phase as long as the tarsal tip touched the ground, and as long as it did not move relative to the ground. Stride length was calculated for each leg as the distance between lift-off and touch-down positions on the ground ('SL' in Fig. 1C). To calculate stride frequency, we divided walking speed by stride length. Different from stride length, stride amplitude was defined as the distance covered by a swing movement of the leg in body coordinates (Wosnitza et al., 2013). Stride amplitude was estimated by subtracting body displacement (swing phase duration × walking speed) from stride length (see also Fig. 1C and Wahl et al., 2015). Swing speed was determined as stride length divided by the duration of the respective swing phase. Angular velocity (deg s^{-1}) was calculated for representative sample steps as the angular deviation of the femur (with respect to body axis) during one swing movement.

We averaged the values recorded in all six legs of an ant to obtain mean values that illustrate general relationships (see Fig. 4A–D), particularly in cases where no significant differences were observed between leg pairs. To illustrate parameters that differed between leg pairs, we calculated mean values for a given pair of legs (L1 and R1; L2 and R2; L3 and R3; Fig. 4E–H; stride amplitude, swing speed and angular velocity).

Phase analysis

To assess the quality of tripod coordination, we calculated tripod coordination strength (TCS) (e.g. Wosnitza et al., 2013). TCS is the ratio of two time periods, t_1/t_2, where t_1 is the time period where all three legs of a given tripod group are simultaneously in swing phase, and t_2 is the time period where at least one of the three legs of the respective tripod group is in swing phase. A TCS value of 1.0 indicates perfect tripod coordination, with all legs in a tripod taking off and touching down simultaneously. The more the TCS value approaches 0, the less synchronous are the swing movements in a tripod group. Phase plots analyse the phase coordination of the six legs in a circular step cycle diagram. The onset of swing (Fig. 5Bi) or stance (Fig. 5Bii) phase in the left hind leg was taken as a reference for the timing of the other five legs. Phase plots were calculated in a MATLAB environment (MathWorks, Inc., Natick, MA, USA) using the 'CircStat' toolbox (Berens, 2009). The duty factor is often used to characterize the transition from walking to running; that is, the introduction of aerial phases into the gait pattern, regarding one leg pair (Alexander, 2003). Duty factor is the duration of the stance phase of a leg divided by the entire duration of the respective step cycle, stance and swing phase together.

Gait analysis

The sequence of swing and stance movements of the six legs was visualized by podograms (Fig. 6A,C). We further quantified the ant's inter-leg coordination by assigning each video frame an index number and a respective index colour, corresponding to the momentary leg coordination observed in that particular video frame (cf. Mendes et al., 2013; Pfeffer and Wittlinger, 2016). Besides the classical gait categories – pentapod, tetrapod, tripod – we also noted the remaining combinations of legs touching the substrate: hexapod, bipod, monopod, aerial phases. For example, in a given video frame, L1, R2, L3 may be in swing phase, and R1, L2, R3 in stance phase. The frame thus shows a typical tripod situation and is assigned index number '3' and colour 'dark green' (see Fig. 6 legend). For a more detailed description of the different categories, see Fig. S3. For the calculation of podograms and frame-by-frame indexing, we used a MATLAB environment (MathWorks).

Statistical comparison

The generation of box-and-whisker plots, normality tests and statistical pairwise and multiple comparisons were performed in SigmaPlot 11.0 (Systat Software Inc., San Jose, CA, USA). Box-and-whisker plots show the median as the box centre, the 25th and 75th percentiles as box margins and the and 90th percentiles as whiskers. Datasets were tested for normal distribution with the Shapiro–Wilk normality test. For pairwise comparisons of normally distributed data, we used the *t*-test; for non-normally distributed data, we used the Mann–Whitney *U*-test (*U*-test). For multiple comparisons of normally distributed data, we used a one-way ANOVA (with Holm–Šidák method as *post hoc* test); for non-normally distributed data, we used an ANOVA on ranks (with Dunn's method as *post hoc* test). Levene's test, realized with Excel (Microsoft Corporation, Remond, WA, USA), was used to compare the variances in footprint positions. For statistical comparisons of circular data, the CircStat toolbox (Berens, 2009) was used. In our figures, a significance level of 0.01 to 0.05 is marked with one asterisk (*), a significance level of 0.001 to <0.01 with two asterisks (**) and a significance level of <0.001 with three asterisks (***).

RESULTS

Cataglyphis desert ants occupy the niche of a thermophilic scavenger that demands a fast and efficient locomotion while foraging. The question of how *C. bombycina* silver ants – renowned for their high speeds – walk across a large range of speeds will be addressed below. To emphasize and explicate particularities of the silver ants' locomotion, we compared their walking behaviour with that of another fast (though not quite as fast) running desert ant species, *C. fortis*.

Journal of Experimental Biology (2019) 222, jeb198705. doi:10.1242/jeb.198705

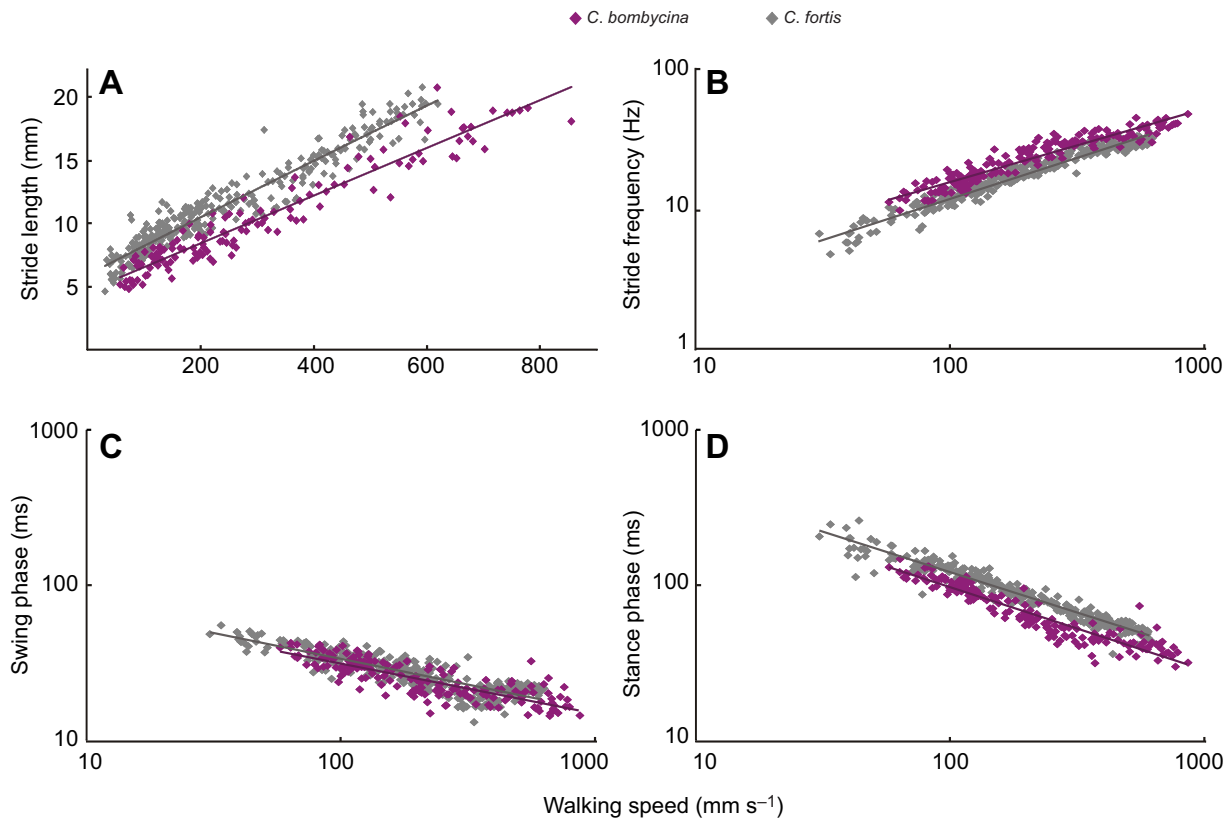

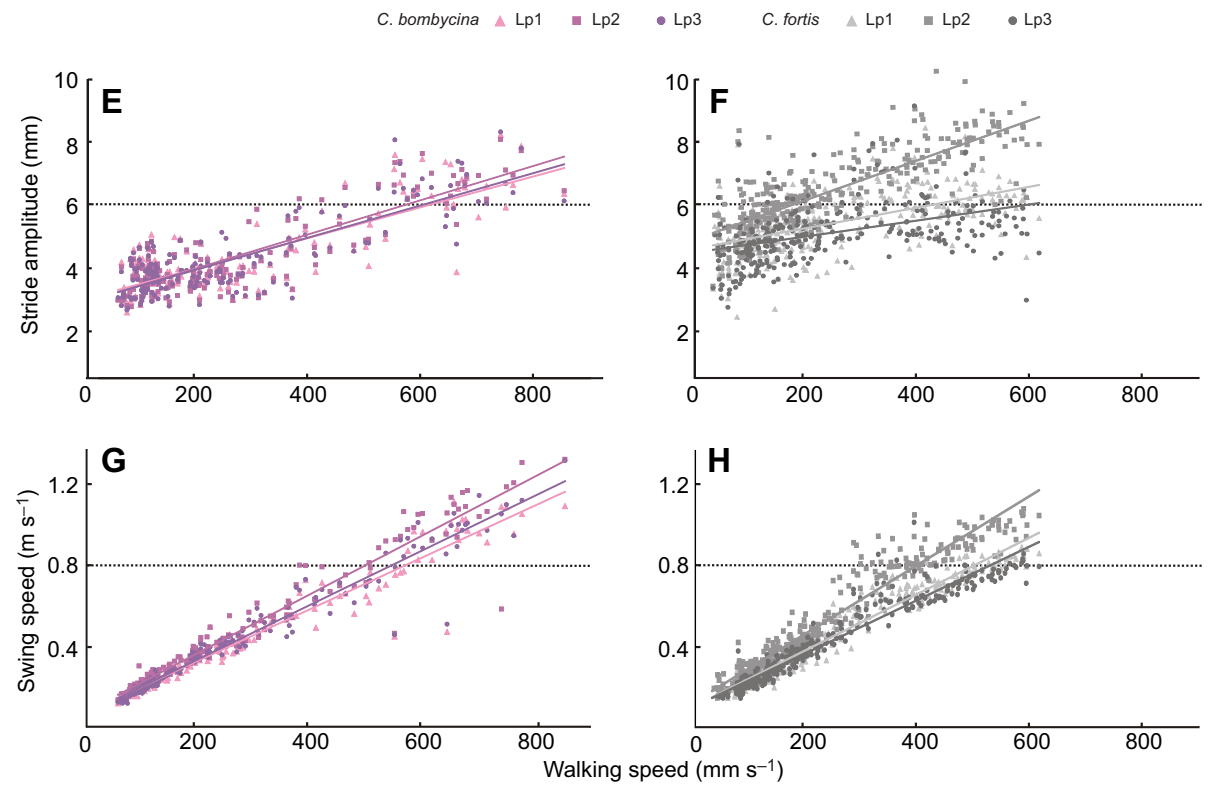

Walking speed	Angular velocity (deg s^{-1}) Lp1	Lp2	Lp3
Slow	421	1379	397
Medium	990	2102	983
Fast	1238	2730	1309

Walking speed	Angular velocity (deg s^{-1}) Lp1	Lp2	Lp3
Slow	368	1336	457
Medium	976	2264	917
Fast	991	2289	926

Fig. 4. See next page for legend.

Fig. 4. Walking parameters. The most significant walking parameters are plotted as functions of walking speed. (A–D) Each data point represents the mean value of all three leg pairs in one video sequence (n=134 for *C. bombycina*; n=305 for *C. fortis*). (A) Stride length (linear regressions: *C. bombycina*, y=0.02x+4.72, R^2=0.91; *C. fortis*, y=0.02x+6.04, R^2=0.92); (B) stride frequency (power functions: *C. bombycina*, y=1.43$x^{0.52}$, R^2=0.90, *C. fortis*, y=0.81$x^{0.59}$, R^2=0.95); (C) swing phase duration (power functions: *C. bombycina*, y=0.14$x^{-0.32}$, R^2=0.69; *C. fortis*, y=0.16$x^{-0.33}$, R^2=0.74); (D) stance phase duration (power functions: *C. bombycina*, y=1.22$x^{-0.80}$, R^2=0.89; *C. fortis*, y=1.58$x^{-0.78}$, R^2=0.94). (E–H) Individual values for the three leg pairs (Lp1, front legs; Lp2, middle legs; Lp3, hind legs). (E) Stride amplitude in *C. bombycina* (linear regressions: Lp1, y=0.0048x+3.02, R^2=0.67; Lp2, y=0.0054x+2.91, R^2=0.73; Lp3, y=0.0051x+2.94, R^2=0.70); (F) stride amplitude in *C. fortis* (linear regressions: Lp1: y=0.0035x+4.42, R^2=0.30; Lp2: y=0.0067x+4.75, R^2=0.63; Lp3: y=0.0027x+4.30, R^2=0.18); (G) swing speed in *C. bombycina* (linear regressions: Lp1, y=1.27x+75.47, R^2=0.95; Lp2, y=1.44x+79.60, R^2=0.94; Lp3, y=1.34x+69.19, R^2=0.95) – table below provides angular velocities during slow (79–82 mm s^{-1}), medium (335–367 mm s^{-1}) and fast (701–855 mm s^{-1}) walking; (H) swing speed in *C. fortis* (linear regressions: Lp1, y=1.48x+71.68, R^2=0.95; Lp2, y=1.80x+86.43, R^2=0.93; Lp3, y=1.40x+69.01, R^2=0.94) – table below provides respective angular velocities during slow (75–81 mm s^{-1}), medium (340–380 mm s^{-1}) and fast (590–620 mm s^{-1}) walking.

Morphometry

For morphometric analyses (Fig. 2) we measured alitrunk length (as proxy of body size; Agosti, 1990) and the length of the different leg pairs for *C. bombycina* and *C. fortis*. The relationships of the different parameters within a species were close to isometry for both species (Fig. S1 and Table S1), as has been demonstrated previously for several desert ants (Sommer and Wehner, 2012). *Cataglyphis bombycina* was statistically significantly smaller than *C. fortis*, regarding all the absolute length measurements. Alitrunk length in *C. bombycina* was 2.5±0.37 mm (12%) shorter, on average, than in *C. fortis*. Leg lengths in *C. bombycina* were even smaller compared with those of *C. fortis*. The first leg pair averaged 4.3 mm (19% shorter), the second leg pair averaged 5.2 mm (18% shorter) and the third leg pair averaged 6.8 mm (18% shorter) than the respective leg pair of *C. fortis*.

Within both species, alitrunk length and leg length showed isometric size relationships. That is, larger individuals had proportionately longer legs, and vice versa. However, *C. bombycina* had shorter legs relative to body size compared with *C. fortis*, despite isometric relationships within the species (Fig. S1 and Table S1).

Footfall geometry and COM

We next analysed the spatial properties of locomotion in *C. bombycina* regarding footfall patterns (Fig. 3). We analysed the footfall patterns of the legs in the PEP, just before lift-off at the end of stance, and in the AEP, just after touch-down at the beginning of stance (Fig. 3A). *Cataglyphis bombycina* showed footfall positions closer to the body when compared with *C. fortis*, consistently in AEPs and PEPs of all legs. This observation is indicative of the relatively shorter legs and the slightly more flexed leg conformation in the *C. bombycina* ants (see example videos: doi:10.13140/RG.2.2.21093.45282 and doi:10.13140/RG.2.2.12704.84488). The tarsal contact areas showed no significantly larger variability in *C. bombycina* than in *C. fortis*, indicated by the separate evaluation of footfall clustering in Fig. 3B. Intriguingly, COM movement can be described by a steady walking path with no apparent variation in speed or acceleration in the rhythm of the step cycle, either for longitudinal or for transverse horizontal COM movements (see Figs S4 and S5).

In comparison to *C. fortis*, *C. bombycina* thus have their tarsal ground contacts closer to the body. This is true not only in absolute terms but also explicitly for measurements normalized to body dimensions.

Walking parameters

General walking parameters were analysed in the natural range of locomotor speeds, from 57 to 855 mm s^{-1} for *C. bombycina* and from 30 to 620 mm s^{-1} for *C. fortis*. The results presented below are summarized in Fig. 4, and the corresponding regression line equations with slope and intercept values are stated in the figure legend.

With increasing walking speed, stride length (Fig. 4A) increased from 4.7 mm (at 73 mm s^{-1}) to 20.8 mm (at 618 mm s^{-1}) in *C. bombycina*; that is, stride length more than quadrupled. Not surprisingly, because of their longer legs, *C. fortis* showed larger stride lengths at the respective walking speeds. However, the slopes of the linear regression lines (*C. bombycina*: y=0.02x+4.72; *C. fortis*: y=0.02x+6.04) and the range of stride lengths (4.5–21 mm) were quite comparable between the two species. Note that in both ant species the natural limit of stride length was further increased by the insertion of aerial phases that started to emerge in *C. fortis* at around 350 mm s^{-1}, and in *C. bombycina* at around 150 mm s^{-1} (compare Fig. 6, 'aerial phase' category in gait analysis; and Fig. 5C,D graphs intersecting 0.5 duty factor line).

With increasing walking speed, stride frequency (Fig. 4B) increased following a power function, although with different slopes in the two species (power functions for *C. bombycina*: y=1.43$x^{0.52}$; *C. fortis*: y=0.81$x^{0.59}$). In silver ants, stride frequency levelled off beyond speeds of 150–200 mm s^{-1} towards a value of 40 Hz. The highest stride frequencies of up to 47 Hz observed in *C. bombycina* (at 855 mm s^{-1}), exceeded the frequency plateau recorded in *C. fortis* at about 30 Hz. The highest measured frequency in *C. fortis* was 36 Hz at 596 mm s^{-1}.

Swing and stance phase durations (Fig. 4C,D) shortened with increasing walking speed in both ant species. At low walking speeds, stance phase duration was longer than swing phase duration; at medium and high walking speeds, this relationship reversed – that is, swing phase was longer than stance phase. The reversal point, with phase durations being about equal, was at a walking speed of about 100 mm s^{-1} in *C. bombycina* and about 180 mm s^{-1} in *C. fortis*. Notably, at high walking speeds, the silver ants' stance and swing phase durations decreased below those observed in *C. fortis*. Swing phase in *C. bombycina* exhibited a minimum duration of 17 ms and thus was just slightly shorter than the 19 ms recorded in *C. fortis*. Stance phase duration was as short as 7 ms in *C. bombycina*, while the minimum duration in *C. fortis* was almost twice as long, at 12 ms.

Stride amplitude (Fig. 4E,F) represents the size of a swing movement relative to body coordinates (see Materials and Methods). It thus indicates by how much a leg's swing movement exceeds the respective body movement during the swing. Stride amplitude increased linearly with walking speed, from 2.5 mm at 73 mm s^{-1} to 8 mm at 742 mm s^{-1} in *C. bombycina*, and from 2.0 mm at 74 mm s^{-1} to 10.4 mm at 433 mm s^{-1} in *C. fortis*. The shorter leg lengths of *C. bombycina* (cf. Fig. 2) are reflected in the smaller maximum stride amplitude. The similar slopes of the stride amplitude versus walking speed regression lines (Fig. 4E) indicate correspondingly similar performance of the three leg pairs in *C. bombycina*. In *C. fortis*, by contrast, a special role of the middle legs (Fig. 4F), probably related to propulsion and perhaps steering, has been discussed previously (Wahl et al., 2015).

The velocity of leg movements rose with increasing walking speed in an almost linear fashion, indicated by swing speed (Fig. 4G,H) and by corresponding angular velocities of the femur (table below Fig. 4G,H). Regression lines of the swing speed versus walking speed

Journal of Experimental Biology (2019) 222, jeb198705. doi:10.1242/jeb.198705

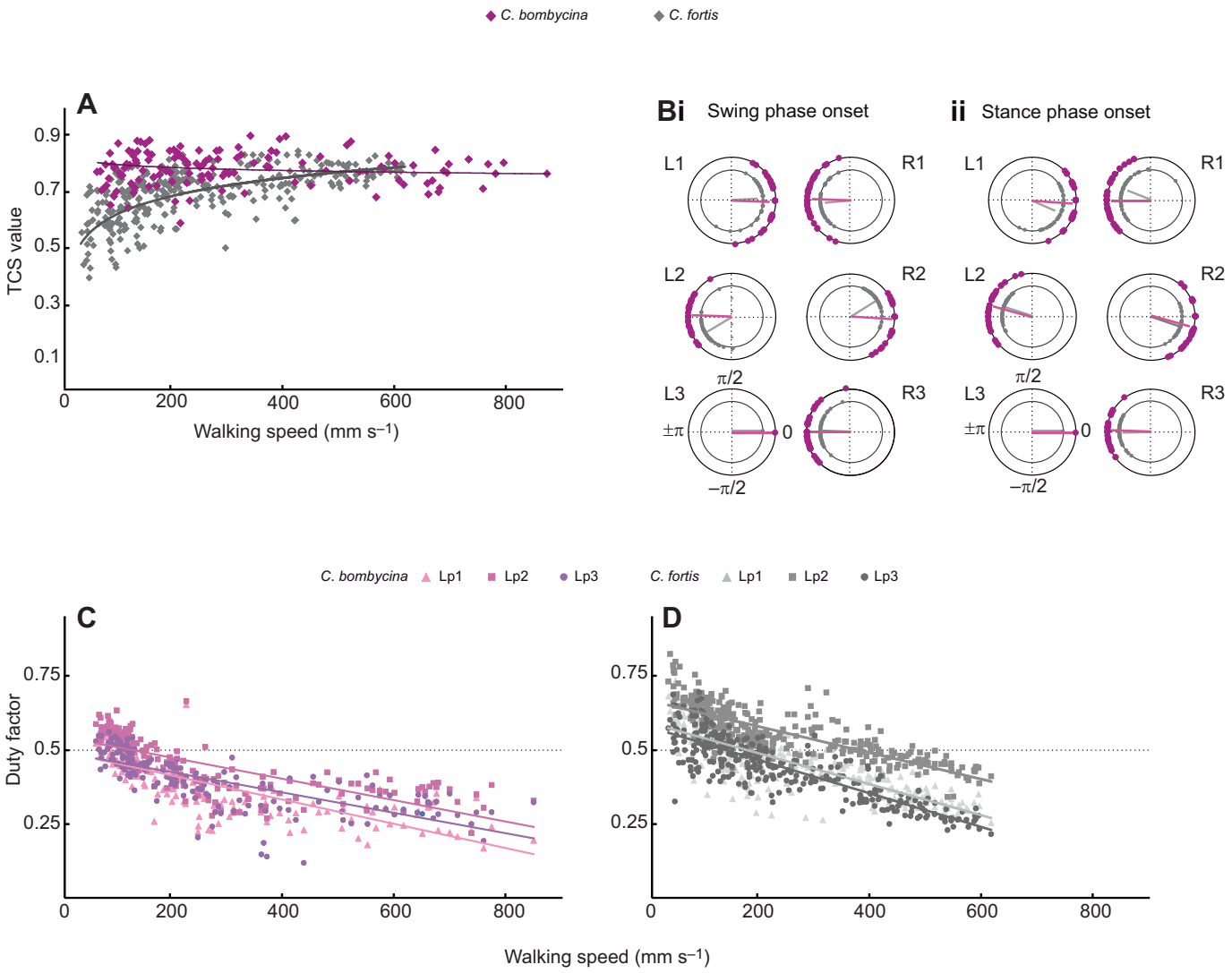

Fig. 5. Leg coordination parameters. (A) Mean tripod coordination strength (TCS, see Materials and Methods) plotted as a function of walking speed (logarithmic regression: *C. bombycina*, $y=-0.015\ln x+0.85$, $R^2=0.02$; *C. fortis*, $y=0.097\ln x+0.18$, $R^2=0.46$). (B) Phase relationships of the six legs analysed for *C. bombycina* (violet; circle represents 30.3 ms) and *C. fortis* (grey; circle represents 35.6 ms) with regard to swing phase onset (Bi) and stance phase onset (Bii). Cycle phase rotates counter-clockwise. The left hind leg (L3) served as reference (phase 0). For each species, 20 videos (60 step cycles) were analysed at speeds from 300 to 400 mm s^{-1}. Each data point represents the onset of swing or stance with respect to L3. The length of the mean phase vector indicates the variance of data points. Statistically significant differences between the two species emerged during swing onset (Bi) for L2 (Kuiper two-sample test, $P=0.002$) and R2 (Kuiper two-sample test, $P=0.001$) with a time shift of around 3.3 ms, as well as during stance phase onset (Bii) for L1 and R1 (Kuiper two-sample test, both with $P=0.05$) with a time shift of about 2.6 ms. (C,D) Duty factor plotted as a function of walking speed for the three leg pairs in (C) *C. bombycina* (linear regressions: Lp1, $y=-0.0004x+0.49$, $R^2=0.61$; Lp2, $y=-0.0004x+0.54$, $R^2=0.56$; Lp3, $y=-0.0003x+0.49$, $R^2=0.54$) and (D) *C. fortis* (linear regressions: Lp1: $y=-0.0005x+0.59$, $R^2=0.66$; Lp2: $y=-0.0004x+0.66$, $R^2=0.61$; Lp3: $y=-0.0006x+0.57$, $R^2=0.73$).

graphs tended to exhibit slightly lower slopes in *C. bombycina*. The fastest absolute swing speeds of 1.3 m s^{-1} were not reached by *C. fortis*, however. A striking characteristic of desert ant locomotion appears to be the middle legs performing the fastest swing movements, spending less time in the air than the front and hind legs, and therefore showing the highest duty factor (see Fig. 5B–D).

In summary, *C. bombycina* apparently reaches high running speeds by having high stride frequencies of more than 40 Hz. These high frequencies are achieved by very short stance phases and fast swing speeds. The shorter legs, and resulting smaller stride lengths, of *C. bombycina* appear to be compensated for in this way.

Phase analysis

TCS (Fig. 5A) captures the synchrony of leg swing movements in a tripod group; that is, one middle leg and the contralateral front and hind legs. TCS thus provides a measure of tripod gait quality (Wosnitza et al., 2013), with values of 1.0 characterizing exact synchrony in the movements of the legs in a tripod. In *C. bombycina*, TCS values were remarkably constant across the whole walking speed range. Observed values were mostly between 0.7 and 0.9, clustering around 0.8. These values were higher than TCS values recorded in *C. fortis*, especially at slow walking speeds.

Stance and swing movements are repetitive events in the step cycle. A circular illustration is thus an adequate means to analyse variability of inter-leg coordination. Phase plots show the onsets of swing (Fig. 5Bi) and stance (Fig. 5Bii) during the step cycle, with the left hind leg (L3) serving as reference (and thus without data point scatter in the diagrams). Considering the TCS values reported above, it was not surprising to observe a clear anti-phase relationship between the two tripod groups, L1, R2, L3 and R1,

Journal of Experimental Biology (2019) 222, jeb198705. doi:10.1242/jeb.198705

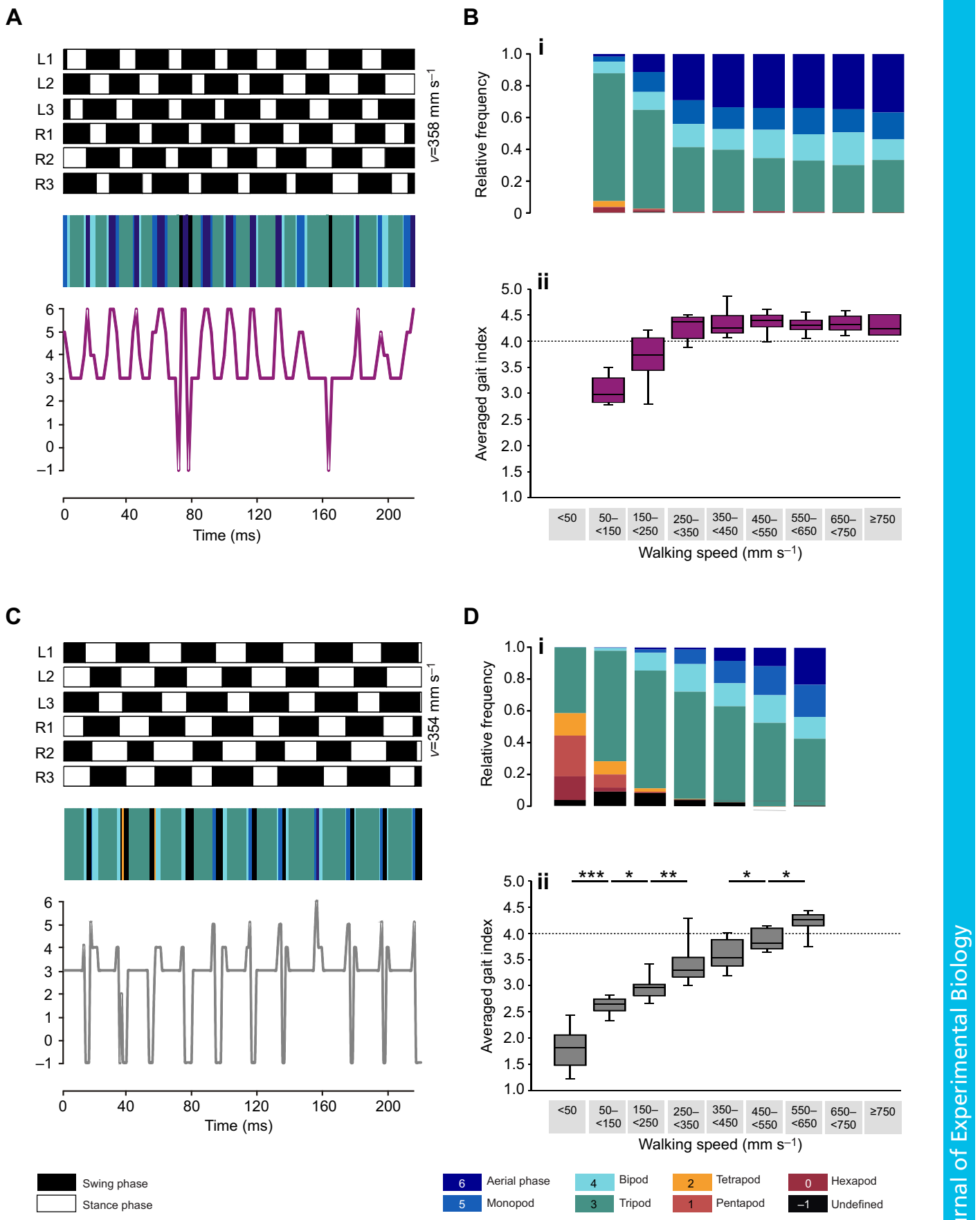

Fig. 6. See next page for legend.

Fig. 6. Podograms and quantification of gait patterns. (A,C) Sample podograms (top) recorded in *C. bombycina* (A) and *C. fortis* (C) at similar walking speeds (about 350–360 mm s^{-1}), and the corresponding colour (middle) and number indices (bottom) plotted along the same time axis. Podograms illustrate the footfall patterns of the six legs; black bars indicate swing and white bars indicate stance phases (L, left; R, right body side; 1, 2 and 3, front, middle and hind legs). Each frame in the video was assigned a colour (middle) and a number index (bottom) according to leg coordination in the particular frame (see colour and number code keys at the bottom of the figure). (B,D) Quantitative analyses according to walking speed class (<50 to >750 mm s^{-1}) for *C. bombycina* (B; n=71) and *C. fortis* (D; n=70). No data were available for the <50 mm s^{-1} speed class in *C. bombycina*, and for the 650 to <750 mm s^{-1} and ≥750 mm s^{-1} speed classes in *C. fortis*. Colour index analyses (Bi,Di) are shown as normalized frequency plots, and number index data (Bii,Dii) as averaged index numbers (ordinates) for the respective walking speed bins (abscissae). *Cataglyphis bombycina* reaches its maximum gait index beyond about 250 to <350 mm s^{-1}; there were no statistically significant differences (of neighbouring speed bins) as indicated by the results of an ANOVA on ranks. *Cataglyphis fortis* shows a gradual increase in the number indices over the entire walking speed range; there were statistically significant differences between neighbouring speed bins (one-way ANOVA): <50 mm s^{-1} and 50 to <150 mm s^{-1} (***P≤0.001); 50 to <150 mm s^{-1} and 150 to <250 mm s^{-1} (*P≤0.017); 150 to <250 mm s^{-1} and 250 to <350 mm s^{-1} (**P=0.010); 350 to <450 mm s^{-1} and 450 to <550 mm s^{-1} (*P=0.025); 450 to <550 mm s^{-1} and 550 to <650 mm s^{-1} (*P=0.013).

L2, R3. Swing and stance phase onset of the three legs in a tripod group occurred almost simultaneously. Although clear tripod coordination was obvious in both ant species, there were small differences regarding the relative timing of the different legs within the step cycle. In *C. bombycina*, all three legs were lifted off (onset of swing phase) and put down on the ground (onset of stance phase) in almost perfect synchrony, except for the stance phase onset of the middle legs. The middle legs were lifted together with the front and hind legs of their tripod group, but they started the transition towards stance phase slightly earlier (1.7 ms) than the front and hind legs.

Cataglyphis fortis, by comparison, showed larger relative phase shifts regarding all leg movements during the step cycle, as indicated by lower TCS values. This resulted in a not quite synchronous transition between swing and stance phases of the legs in one tripod group. There was a clear tendency for the hind leg in a tripod to be lifted off the ground first, followed by the front leg and the middle leg performing stance–swing transition last. For the swing–stance transition, the front and middle legs touched down in near synchrony, while the hind leg was the last to terminate its swing phase.

The duty factor represents that fraction of step cycle duration that is occupied by the stance phase, when the body is supported by a given leg. When the duty factor drops below 0.5, the swing phases of a given leg pair overlap as the stance phases of the two legs cannot cover the whole step cycle period. This is the reason why the duty factor is often used to characterize the transition from walking to running, especially for bipedal runners (see Discussion).

With increasing walking speed, duty factor decreased in all three leg pairs, although in a somewhat different manner in the two ant species (Fig. 5C,D). In *C. bombycina*, the front and hind leg duty factor dropped below 0.5 at rather low walking speeds, below 100 mm s^{-1}. The middle legs assumed a duty factor below 0.5 last, indicative of the final transition from walking to running, at about 120 mm s^{-1}. In *C. fortis*, these transitions occurred at much higher speeds, at about 170 mm s^{-1} for front and hind legs, and at a remarkable speed of about 370 mm s^{-1} for the middle legs.

In summary, leg movements in a tripod group are well synchronized in *C. bombycina*, even at low walking speeds, and aerial phases occur at remarkably low walking speeds of about 120 mm s^{-1}.

Gait analysis

We characterized the silver ants' walking behaviour by further gait analyses. Fig. 6A shows an example of a podogram and corresponding gait indexing for *C. bombycina*; Fig. 6C provides an example for *C. fortis*, recorded at similar walking speeds (about 350 mm s^{-1}). Podograms present the alternation between swing and stance phases over time as black (swing) and white (stance) bars. For a quantitative analysis, each frame of the video was assigned an index number and a colour code marking the leg coordination in the particular video frame (see Fig. 6 legend; Fig. S3). *Cataglyphis bombycina* showed a consistent use of aerial phase (Fig. 6B, number code '6', colour code 'dark blue') above walking speeds of 250 mm s^{-1}, while this was an altogether rarer event in *C. fortis*, except at the very highest speeds (Fig. 6D).

The method of gait indexing was used to quantify gait patterns across the observed range of walking speeds in both *C. bombycina* (Fig. 6B) and *C. fortis* (Fig. 6D). Gait indexing does not consider a continuous gait, such as a tripod gait, but rather assigns each frame in a video recording an index number according to the momentary leg coordination in that frame (see Fig. 6 legend). In *C. fortis*, there was a continuous change in gait pattern composition across the entire walking speed range, from the <50 mm s^{-1} bin to the <650 mm s^{-1} bin (Fig. 6Bi). Statistically significant changes in gait representation occurred between all adjacent speed bins except one (see Fig. 6 legend). In *C. bombycina*, by contrast, there were changes in gait pattern composition only from the lowest walking speeds up to the 250 to <350 mm s^{-1} speed bin (Fig. 6Bi). For higher walking speeds, no statistically significant changes in the relative frequency of gait patterns were observed, with the silver ants exhibiting rather constant proportions of gait patterns. Aerial phases accounted for about 30%, periods with more than three legs in swing phase and monopod or bipod coordination for about 15% each, and tripod coordination for about 40%.

This was also indicated by a consistently high mean index number of about 4.3 (Fig. 6Bii, index number of 4, marking bipod coordination, and 5, indicating monopod coordination). In *C. fortis*, by comparison (Fig. 6Dii), there was a large proportion of gait patterns with more than three legs in stance phase at the lowest speeds (<50 mm s^{-1}): hexapod 15%, pentapod 26%, tetrapod 14%, with a mean index number of 1.7. The gait composition changed gradually towards patterns with at least three legs in swing phase: tripod 43%, bipod 14%, monopod 20%, aerial phases 23%, with a mean index number of 4.2 in the highest speed bin (550 to <650 mm s^{-1}). Thus, only at the highest speeds was the gait pattern composition similar to that of *C. bombycina*.

In summary, *C. bombycina* consistently employs gait patterns with at least three legs in the air, i.e. tripod, bipod, monopod or aerial phases, across most of its walking speed range. Aerial phases occur at intriguingly low walking speeds, with almost 15% at 150 mm s^{-1} and about 30% above that speed. This is achieved by overlapping swing movements of the two tripod groups, partly as a result of the high synchrony of the leg movements within a tripod.

DISCUSSION

Cataglyphis bombycina (Wehner et al., 1992) and *Cataglyphis fortis* are sister desert ant species that inhabit North African sand dune and salt pan habitats, respectively, but are quite similar otherwise. An intriguing difference concerns relative leg length, which is shorter in *C. bombycina* despite the fact that this species achieves higher walking speeds. This was the initial incentive for the present analysis, where we observed a number of distinct differences in the details of the two species' walking behaviour.

Relative walking speed

We were able to measure top absolute walking speeds of 855 mm s^{-1} in *C. bombycina*, a value that comes close to the maximum running speeds of 1 m s^{-1} recorded previously (Wehner, 1983) with different methods. Calculating relative walking speed, typically in body lengths per second, appears more adequate when analysing parameters related to body size such as stride length or stride amplitude. *Cataglyphis bombycina* achieves maximum relative speeds of about 108 body lengths per second (which is around 157 leg lengths per second), one of the highest values documented for running animals. It is outperformed according to our present knowledge by very few species, most notably a Californian coastal mite (*Paratarsotomus macropalpis*) and an Australian tiger beetle (*Cicindela* sp.), with relative speeds of up to 377 and 171 body lengths per second, respectively (Rubin et al., 2016; Kamoun and Hogenhout, 1996).

Parameters contributing to high walking speeds

From an evolutionary perspective, low food density and a hot climate in the North African deserts exert selective pressures that make fast and efficient foraging a crucial feat for the scavenging silver ants (Wehner and Wehner, 2011). To achieve high walking speeds, virtually all legged animals optimize spatial and temporal parameters (Heglund et al., 1974; Heglund and Taylor, 1988) that we have addressed in the present study. Although one might expect that the two examined ant species, *C. bombycina* and *C. fortis*, use the same strategies to reach high walking speeds, our analysis revealed distinct differences in the way the two species use those spatial and temporal parameters, as discussed below.

Absolute leg length per se would appear to limit stride length in *C. bombycina*, unless stride length is increased by inserting aerial phases into the walk. Maximum absolute stride length is quite similar at 20.81 mm in *C. bombycina* (at 618 mm s^{-1}) and 20.84 mm in *C. fortis* (at 592 mm s^{-1}). Interestingly, this holds true when calculating maximum relative stride length (stride length/alitrunk length), resulting in 2.34 and 2.41 for *C. bombycina* and C. *fortis*, respectively. This means that silver ants, with their shorter bodies and even shorter legs, enlarge their range of stride lengths by inserting aerial phases. They do this to a larger extent than *C. fortis*, a fact that was further demonstrated by measuring stride amplitude. *Cataglyphis fortis* ants exhibited larger stride amplitudes than *C. bombycina*, suggesting that they exploit their leg span without inserting aerial phases up to larger stride lengths and walking speeds than *C. bombycina*.

To achieve high stride frequencies, *C. bombycina* ants reduce step cycle period by shortening primarily stance phase duration, to a minimum of 7 ms. This is almost half the minimum stance phase duration in *C. fortis* of 12 ms. Swing phase duration is reduced relatively less, to a minimum of 17 ms in *C. bombycina*. This is slightly below the minimum of 19 ms in *C. fortis*. A steeper decline of stance phase duration compared with swing phase duration with increasing walking speed is commonly observed in walking animals (e.g. in stick insects: Wendler, 1964). This is due to the fact that swing phases are performed without mechanical load that relates to walking speed.

As noted above, only a few animals are known to achieve higher stride frequencies than *C. bombycina*, including the mite *Paratarsotomus macropalpis* (Rubin et al., 2016). These animals are much smaller than ants, about 0.7 mm in body length, and stride frequencies are correspondingly faster, ranging above 100 Hz. Together, this results in the mites moving at very low Reynolds numbers, between 4 and 5. Depending on body length, walking speed and ambient temperature, Reynolds numbers for *C. bombycina* range from about 140 (for an 8 mm ant walking at a medium speed of 300 mm s^{-1} at 45°C) to 570 (for an 11 mm ant walking at the maximum speed of 840 mm s^{-1} and a moderate temperature of 30°C). These Reynolds numbers are typically relevant for small flying insects, such as small *Drosophila* species. Viscous forces, rather than inertial momentums of the legs, would thus appear to impose speed limits.

Stride frequency is restricted by muscle contraction and relaxation kinetics (Rubin et al., 2016). In this context, the short legs of *C. bombycina* – by long-legged *Cataglyphis* standards – may be significant for reaching high leg movement speeds and high stride frequencies, as reported here. After all, long legs have high momentums of inertia, in small arthropods as well as in large mammals (Heglund et al., 1974; Heglund and Taylor, 1988). The relatively short legs may thus contribute to *C. bombycina* reaching a 40 Hz stride frequency, while the longer-legged *C. fortis* achieves just about 30 Hz.

Notably, this result is in accordance with the model of the spring-loaded inverted pendulum (SLIP), which abstracts the alternating movement of two coupled tripod leg groups as a spring-mass monopod (Blickhan and Full, 1993). The SLIP model nicely shows that smaller individuals change gait at lower walking speeds and show generally higher stride frequencies. Both aspects were observed in the present comparison of ant species. The smaller ant, *C. bombycina*, introduces aerial phases at lower walking speeds and reaches higher stride frequencies than its larger sister, *C. fortis*.

Leg coordination and gait patterns

Leg coordination parameters are of secondary importance for speed production, but they are of course essential for static and dynamic stability (e.g. Ting et al., 1994). Several idealized gaits are known in insects – pentapod, tetrapod, tripod – merging into one another in a speed-dependent gait continuum (Wilson, 1966; Schilling et al., 2013; Dürr et al., 2018). A typical low-speed walking pattern is pentapod coordination, also termed wave gait, with one leg in swing and five legs on the ground. At intermediate walking speeds, tetrapod coordination is often observed, with two diagonally arranged legs in the air and four legs, supporting the body. For fast walking speeds, tripod coordination is typically observed, with three legs simultaneously in swing and three legs in stance phase, coupling the front and hind legs of one body side and the middle leg of the other body side into a tripod group.

Stick insects are textbook examples demonstrating the entire spectrum of the gait continuum from pentapod to tetrapod to tripod coordination with increasing walking speed (Wilson, 1966; Graham, 1972). The concept of gait continuum has been linked to several coordination rules derived from behavioural experiments (Cruse, 1990; Dürr et al., 2018) that were verified by successful implementation in hexapod walking models and machines (Schilling et al., 2013). Many insects, and especially faster walking species, apparently occupy just the upper end of the gait continuum, including cockroaches, beetles and ants (Hughes, 1952; Bender et al., 2011; Zollikofer, 1994). In these animals, the gait continuum is extended beyond the tripod by insertion of aerial phases (via bipod and monopod situations as tripod pattern variations), allowing higher walking speeds.

Note, however, that the definition of traditional walking patterns (pentapod, tetrapod, tripod) is based on the coupling of particular legs in the step cycle, while the extension of the gait continuum beyond the tripod gait that has been applied here (bipod, monopod, aerial phases) is the result of the continuous (and increasing) overlap of the swing phases of the two tripod groups. For strict and fast-walking tripod walkers, it would appear favourable to extend the

gait continuum from exact tripod coordination (three legs in the air, three legs on the ground), via bipod (four legs in swing, two legs in stance) and monopod (five legs in swing and one leg in stance) coordination to aerial phases (all six legs in the air, with one tripod just after lift-off, the other just before touch-down; see also Fig. S3). This characterization appears to be a useful way to achieve a quantitative temporal analysis for the description of fast locomotion in hexapods.

Leg synchrony and aerial phases

A striking characteristic of the silver ant's locomotion is the high synchrony of the step cycles in the legs within a tripod group. This is illustrated by the rather constant TCS values of around 0.8 (Fig. 5A) and clearly revealed in phase plot analyses (Fig. 5B). All three legs of a tripod commence swing phase virtually simultaneously, and the middle legs are the first legs to touch down again, with the front and hind legs of the contralateral body side following immediately after. This near synchrony in combination with short stance phase durations leads to the occurrence of aerial phases at remarkably low walking speeds. This is also apparent in the analysis of gait index (Fig. 6) and duty factor (Fig. 5C,D). The middle leg is the last one to decrease its duty factor below 0.5, as an indicator for the occurrence of aerial phases, and it does so at speeds as low as 120 mm s^{-1}, i.e. far lower than in *C. fortis*, where aerial phases occur at about 370 mm s^{-1} and above. In the silver ant, aerial phases thus occur well before maximum stride lengths or stride frequencies are reached. Duty factor is an indirect indicator of the occurrence of aerial phase, compared with gait indexing, for example. Regarding a single pair of legs, a duty factor below 0.5 implies that swing phase accounts for more than half of step cycle duration, resulting in swing phase overlap in that particular leg pair. However, in hexapods, and even quadrupeds, this does not imply the simultaneous occurrence of swing phase overlap in all leg pairs. High synchrony of the legs in a tripod results in a walking pattern in *C. bombycina* that is strongly reminiscent of bipedal locomotion, though, with the alternating tripods representing the two legs. This makes the duty factor a quite useful concept for the present study.

Synchronization of legs can lead to aerial phases (as a classical definition for the walk–run transition; Hildebrand, 1985), appropriate to several arthropods such as *Periplaneta americana* (Full and Tu, 1991), ghost crabs (Burrows and Hoyle, 1973) or *Hololena* spiders (Spagna et al., 2011). Other fast running arthropods do not show such high synchronization [e.g. the cockroach *Blaberus discoidalis* (Full and Tu, 1991), *Formica* wood ants (Reinhardt and Blickhan, 2014)]. To determine the walk–run transition in these cases, in the absence of aerial phases, further analysis is required such as ground reaction force patterns, energy transfer between the legs and body, and energy fluctuation patterns of the COM. These criteria have never been applied to desert ant locomotion, to our knowledge, but they exceed the scope of the present study and our current dataset.

As for the two *Cataglyphis* species, different arthropod taxa appear to behave differently at high speeds, with some tending towards more metachronal patterns and some species strengthening the synchronization of leg swings (which might require specific features for elastic energy storage in the legs; Weihmann et al., 2017; Weihmann, 2018). In line with the SLIP model (Blickhan and Full, 1993), leg synchronization in *C. bombycina* increases vertical forces and vertical amplitudes of the COM which might lead to increased elastic energy storage in the legs. Pronounced synchronization would appear favourable as all three tripod legs contribute equally to acceleration on the sand substrate. Movement of the COM in this context appears to be restricted to the vertical plane. Our high-speed videos taken in top view demonstrate movement of the alitrunk along a remarkably straight path at similarly remarkable constant speed (see Figs S4 and S5).

Adaptations to the sand dune habitat

In the present study, we demonstrated that two closely related desert ants, namely *C. bombycina* and *C. fortis*, exhibit intriguing differences regarding their walking behaviour. One reason why silver ants may have evolved their peculiar locomotor behaviour is the Saharan dune habitat, as opposed to the hard-baked clay in salt pans habitat of *C. fortis*. This concerns in particular *C. bombycina*'s combination of high stride frequencies, short stance phases and fast swing movements in achieving high running speeds, together with the high synchrony of the legs in a tripod. There are two related potential advantages of this leg movement pattern.

First, this coordination results in brief, synchronous and forceful impacts of three legs on the sand substrate, which may serve to minimize sinking into the yielding dune sand (Li et al., 2009). After all, brief and fast movements in these small animals should occur at low Reynolds numbers and high substrate viscosity. The smaller body size, and thus body mass, of *C. bombycina* compared with *C. fortis* may further help to reduce the ants' subsidence into the soft granular medium.

Second, the high synchrony in the leg movements of a tripod should distribute body mass rather evenly across the tripod. A rather even distribution of body mass among the three legs of a tripod should be advantageous for both touch-down and lift-off. Both transitions will require relatively high acceleration forces when considering the brief stance phase durations (cf. Zollikofer, 1988).

Acknowledgements

We thank Annette Christine Janssen, Tanja Kaiser and Alexander Schaarmann for their most dedicated help with the field work, laboratory experiments and high-speed video analysis. Wolfgang Mader deserves sincere thanks for his help with statistical evaluations, and Alexander Lindt and Andrea Kubitz for their support in animal care. Ursula Seifert helped with editing and correcting the English in the manuscript. We thank Rüdiger Wehner and Stefan Sommer for providing morphological data for *C. fortis*.

Competing interests

The authors declare no competing or financial interests.

Author contributions

Conceptualization: S.E.P., V.L.W., M.W., H.W.; Investigation: S.E.P., V.L.W.; Data curation: V.L.W.; Writing - original draft: S.E.P., V.L.W.; Writing - review & editing: H.W.; Visualization: S.E.P.; Supervision: M.W., H.W.; Project administration: M.W.

Funding

The University of Ulm provided basic financial support and infrastructure.

Data availability

High-speed videos of *Cataglyphis bombycina* and *Cataglyphis fortis* locomotion are available from ResearchGate: doi:10.13140/RG.2.2.21093.45282 and doi:10.13140/RG.2.2.12704.84488

Supplementary information

Supplementary information available online at
http://jeb.biologists.org/lookup/doi/10.1242/jeb.198705.supplemental

References

Agosti, D. (1990). Review and reclassification of *Cataglyphis* (*Hymenoptera, Formicidae*). *J. Nat. Hist.* **24**, 1457-1505. doi:10.1080/00222939000770851

Alexander, R. M. (2003). *Principles of Animal Locomotion*. New Jersey, USA: Princeton University Press.

Bender, J. A., Simpson, E. M., Tietz, B. R., Daltorio, K. A., Quinn, R. D. and Ritzmann, R. E. (2011). Kinematic and behavioral evidence for a distinction between trotting and ambling gaits in the cockroach *Blaberus discoidalis*. *J. Exp. Biol.* **214**, 2057-2064. doi:10.1242/jeb.056481

Berens, P. (2009). CircStat: a MATLAB toolbox for circular statistics. *J. Stat. Softw.* **31**, 1-21. doi:10.18637/jss.v031.i10
Blickhan, R. and Full, R. J. (1993). Similarity in multilegged locomotion: bouncing like a monopode. *J. Comp. Physiol. A* **173**, 509-517. doi:10.1007/BF00197760
Burrows, M. and Hoyle, G. (1973). The mechanism of rapid running in the ghost crab, *Ocypode ceratophthalma*. *J. Exp. Biol.* **58**, 327-349.
Cruse, H. (1990). What mechanisms coordinate leg movement in walking arthropods? *Trends Neurosci.* **13**, 15-21. doi:10.1016/0166-2236(90)90057-H
Dürr, V., Theunissen, L. M., Dallmann, C. J., Hoinville, T. and Schmitz, J. (2018). Motor flexibility in insects: adaptive coordination of limbs in locomotion and near-range exploration. *Behav. Ecol. Sociobiol.* **72**, 15-21. doi:10.1007/s00265-017-2412-3
Full, R. J. and Tu, M. S. (1991). Mechanics of six-legged runners. *J. Exp. Biol.* **148**, 129-146.
Gehring, W. J. and Wehner, R. (1995). Heat shock protein synthesis and thermotolerance in *Cataglyphis*, an ant from the Sahara desert. *Proc. Natl. Acad. Sci. USA* **92**, 2994-2998. doi:10.1073/pnas.92.7.2994
Graham, D. (1972). A behavioural analysis of the temporal organisation of walking movements in the 1st instar and adult stick insect (*Carausius morosus*). *J. Comp. Physiol.* **81**, 23-52. doi:10.1007/BF00693548
Heglund, N. C. and Taylor, C. R. (1988). Speed, stride frequency and energy cost per stride: how do they change with body size and gait? *J. Exp. Biol.* **138**, 301-318.
Heglund, N. C., Taylor, C. R. and McMahon, T. A. (1974). Scaling stride frequency and gait to animal size: mice to horses. *Science* **186**, 1112-1113. doi:10.1126/science.186.4169.1112
Hildebrand, D. M. (1985). Walking and running. In *Functional Vertebrate Morphology* (ed. M. Hildebrand D.M. Bramble K.F. Liem and D.B. Wake), pp. 38-57. Cambridge, MA: Belknap Press of Harvard University Press.
Hughes, G. M. (1952). The co-ordination of insect movements. *J. Exp. Biol.* **29**, 267-285.
Kamoun, S. and Hogenhout, S. A. (1996). Flightlessness and rapid terrestrial locomotion in tiger beetles of the *Cicindela* L. subgenus *Rivacindela* van Nidek from saline habitats of Australia (*Coleoptera: Cicindelidae*). *Coleopt. Bull.* **50**, 221-230.
Lenoir, A., Aron, S., Cerda, X. and Hefetz, A. (2009). *Cataglyphis* desert ants: a good model for evolutionary biology in Darwin's anniversary year - a review. *Isr. J. Entomol.* **39**, 1-32.
Li, C., Umbanhowar, P. B., Komsuoglu, H., Koditschek, D. E. and Goldman, D. I. (2009). Sensitive dependence of the motion of a legged robot on granular media. *Proc. Nat. Acad. Sci. USA* **106**, 3029-3034. doi:10.1073/pnas.0809095106
Lighton, J. R. B. and Wehner, R. (1993). Ventilation and respiratory metabolism in the thermophilic desert ant, *Cataglyphis bicolor* (Hymenoptera, Formicidae). *J. Comp. Physiol. B* **163**, 11-17. doi:10.1007/BF00309660
Mendes, C. S., Bartos, I., Akay, T., Márka, S. and Mann, R. S. (2013). Quantification of gait parameters in freely walking wild type and sensory deprived *Drosophila melanogaster*. *eLife* **2**, e00231. doi:10.7554/eLife.00565
Pfeffer, S. E. and Wittlinger, M. (2016). How to find home backwards? Locomotion and inter-leg coordination during rearward walking of *Cataglyphis fortis* desert ants. *J. Exp. Biol.* **219**, 2110-2118. doi:10.1242/jeb.137778
Reinhardt, L. and Blickhan, R. (2014). Level locomotion in wood ants: evidence for grounded running. *J. Exp. Biol.* **217**, 2358-2370. doi:10.1242/jeb.098426
Rubin, S., Young, M. H.-Y., Wright, J. C., Whitaker, D. L. and Ahn, A. N. (2016). Exceptional running and turning performance in a mite. *J. Exp. Biol.* **219**, 676-685. doi:10.1242/jeb.128652
Schilling, M., Hoinville, T., Schmitz, J. and Cruse, H. (2013). Walknet, a bio-inspired controller for hexapod walking. *Biol. Cybern.* **107**, 397-419. doi:10.1007/s00422-013-0563-5
Seidl, T. and Wehner, R. (2008). Walking on inclines: how do desert ants monitor slope and step length. *Front. Zool.* **5**, 1-15. doi:10.1186/1742-9994-5-8
Shi, N. N., Tsai, C.-C., Camino, F., Bernard, G. D., Yu, N. and Wehner, R. (2015). Keeping cool: Enhanced optical reflection and radiative heat dissipation in Saharan silver ants. *Science* **349**, 298-301. doi:10.1126/science.aab3564
Sommer, S. and Wehner, R. (2012). Leg allometry in ants: extreme long-leggedness in thermophilic species. *Arthropod Struct. Dev.* **41**, 71-77. doi:10.1016/j.asd.2011.08.002
Spagna, J. C., Valdivia, E. A. and Mohan, V. (2011). Gait characteristics of two fast-running spider species (*Hololena adnexa* and *Hololena curta*), including an aerial phase (*Araneae: Agelenidae*). *J. Arachnol.* **39**, 84-91. doi:10.1636/B10-45.1
Ting, L. H., Blickhan, R. and Full, R. J. (1994). Dynamic and static stability in hexapedal runners. *J. Exp. Biol.* **197**, 251-269.
Wahl, V., Pfeffer, S. E. and Wittlinger, M. (2015). Walking and running in the desert ant *Cataglyphis fortis*. *J. Comp. Physiol. A* **201**, 645-656. doi:10.1007/s00359-015-0999-2
Wehner, R. (1983). Taxonomie, Funktionsmorphologie und Zoogeographie der saharischen Wüstenameise *Cataglyphis fortis* (Forel 1902) Stat. *Nov. Senckenbergiana Biol.* **64**, 89-132.
Wehner, R. (1987). Spatial organization of foraging behavior in individually searching desert ants, *Cataglyphis* (Sahara desert) and *Ocymyrmex* (Namib desert). *Exp. Suppl.* **54**, 15-42. doi:10.1111/j.1365-3032.2011.00795.x
Wehner, R. (2016). Early ant trajectories: spatial behaviour before behaviourism. *J. Comp. Physiol. A* **202**, 247-266. doi:10.1007/s00359-015-1060-1
Wehner, R. and Wehner, S. (2011). Parallel evolution of thermophilia: daily and seasonal foraging patterns of heat-adapted desert ants: *Cataglyphis and Ocymyrmex* species. *Physiol. Entomol.* **36**, 271-281. doi:10.1111/j.1365-3032.2011.00795.x
Wehner, R., Marsh, A. C. and Wehner, S. (1992). Desert ants on a thermal tightrope. *Nature* **357**, 586-587. doi:10.1038/357586a0
Weihmann, T. (2018). Leg force interference in polypedal locomotion. *Sci. Adv.* **4**, eaat372. doi:10.1126/sciadv.aat3721
Weihmann, T., Brun, P.-G. and Pycroft, E. (2017). Speed dependent phase shifts and gait changes in cockroaches running on substrates of different slipperiness. *Front. Zool.* **14**, 54. doi:10.1186/s12983-017-0232-y
Wendler, G. (1964). Laufen und Stehen der Stabheuschrecke: Sinnesborsten in den Beingelenken als Glieder von Regelkreisen. *Z. Vgl. Physiol.* **48**, 198-250. doi:10.1007/BF00297860
Willot, Q., Simonis, P., Vigneron, J.-P. and Aron, S. (2016). Total internal reflection accounts for the bright color of the Saharan silver ant. *PLoS ONE* **11**, e0152325. doi:10.1371/journal.pone.0152325
Wilson, D. M. (1966). Insect walking. *Annu. Rev. Entomol.* **11**, 103-122. doi:10.1146/annurev.en.11.010166.000535
Wosnitza, A., Bockemühl, T., Dübbert, M., Scholz, H. and Büschges, A. (2013). Inter-leg coordination in the control of walking speed in *Drosophila*. *J. Exp. Biol.* **216**, 480-491. doi:10.1242/jeb.078139
Zollikofer, C. (1988). Vergleichende Untersuchungen zum Laufverhalten von Ameisen. *PhD thesis*, University of Zürich, Switzerland.
Zollikofer, C. (1994). Stepping patterns in ants-influence of body morphology. *J. Exp. Biol.* **192**, 107-118.

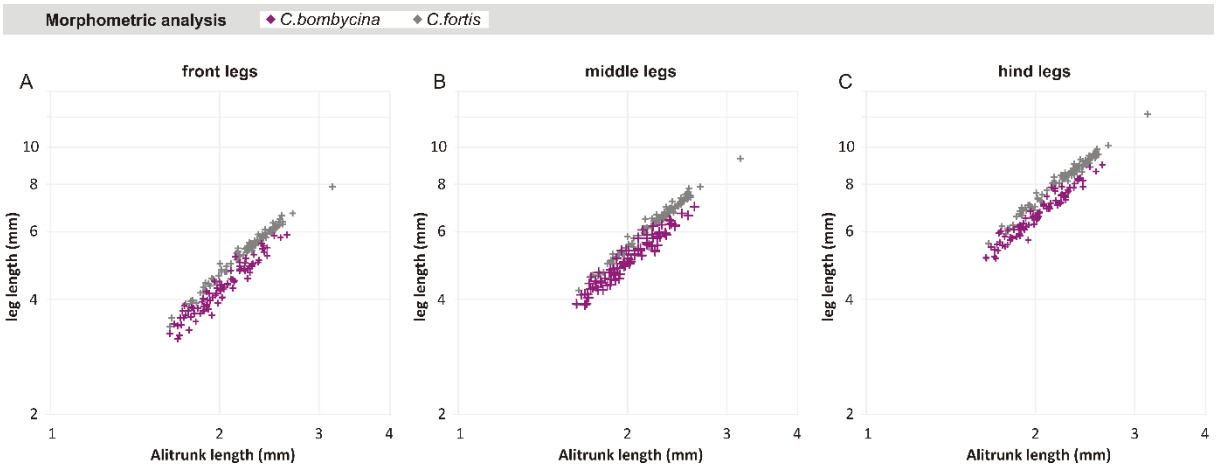

Figure S1 | Relationship between body size (determined as alitrunk length) and leg length in *Cataglyphis* ants. Data are represented as log-log plots for front (**A**), middle (**B**) and hind (**C**) legs for *Cataglyphis bombycina* (lilac, n=86), and *Cataglyphis fortis* (grey, n= 100, data kindly provided by Sommer and Wehner (2012)). Comparing absolute size values, *C. bombycina* was smaller in all size parameters measured. Independent of allometric relationships, leg length increased characteristically from the first to the second to the third leg pair (see Fig. 2), which is in accord with previous findings in a number of other desert ant species (Sommer and Wehner, 2012).

Species	y	a	b	R^2
Cataglyphis bombycina	Front leg	1.6943	1.0383	0.929
	Middle leg	2.1672	0.9694	0.928
	Hind leg	2.9465	0.9254	0.948
Cataglyphis fortis	Front leg	1.8694	1.0286	0.982
	Middle leg	2.2553	1.0115	0.979
	Hind leg	3.1557	0.9403	0.975

Table S1 | Leg allometry values. Values were calculated for the data shown in Figure S1 in the ant species *Cataglyphis bombycina* (n=86) and *Cataglyphis fortis* (n= 100). Parameter estimates are given for the allometric equation $y = a * x^b$, with y and x representing leg length and alitrunk length, respectively. Parameters a and b denote scaling factor and allometric exponent, respectively; R^2 coefficient of determination. To convert the power function into a linear equation we used $\log_{10}$-transformations (i.e. log y = log a + b * log x, note also logarithmic scaling on ordinates and abscissae in Fig. S1 (Warton et al., 2006*)). Allometric coefficient ***'b'*** indicates the slope of the regression line in Fig. S1, capturing the size ratio of leg length and alitrunk lengths. Both *Cataglyphis* species have b-values near 1 (between 0.93 and 1.04), demonstrating isometric scaling between leg and alitrunk lengths within species. That means, smaller individuals have proportionally smaller legs. Parameter ***'log a'*,** represents the intercept of the regression line in Fig. S1. Differences in the intercept between *C. bombycina* and *C. fortis* indicate differences in the proportion between leg and alitrunk lengths. Hence, even in equally sized individuals, leg length would still be smaller in *C. bombycina* than in *C. fortis*.

* **Warton, D. I., Wright, I. J., Falster, D. S., and Westoby, M.** (2006). Bivariate line-fitting methods for allometry. *Biological Reviews* **81**, 259-291.

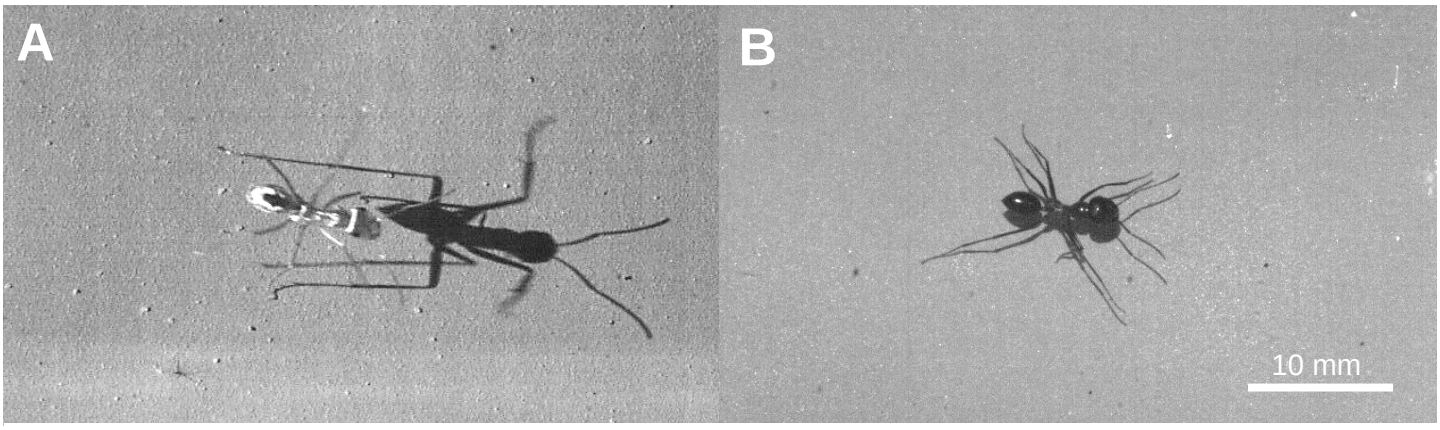

Figure S2 | Sample images from highspeed videos. (**A**) *C. bombycina* (supplementary video V1, recorded with 500 Hz) and (**B**) *C. fortis* (supplementary video V2, recorded with 1000 Hz) during locomotion. Scale bar equal for **(A**) and (**B**); videos are also available on research gate website ((A) DOI: 10.13140/RG.2.2.21093.45282 (B) DOI: 10.13140/RG.2.2.12704.84488)

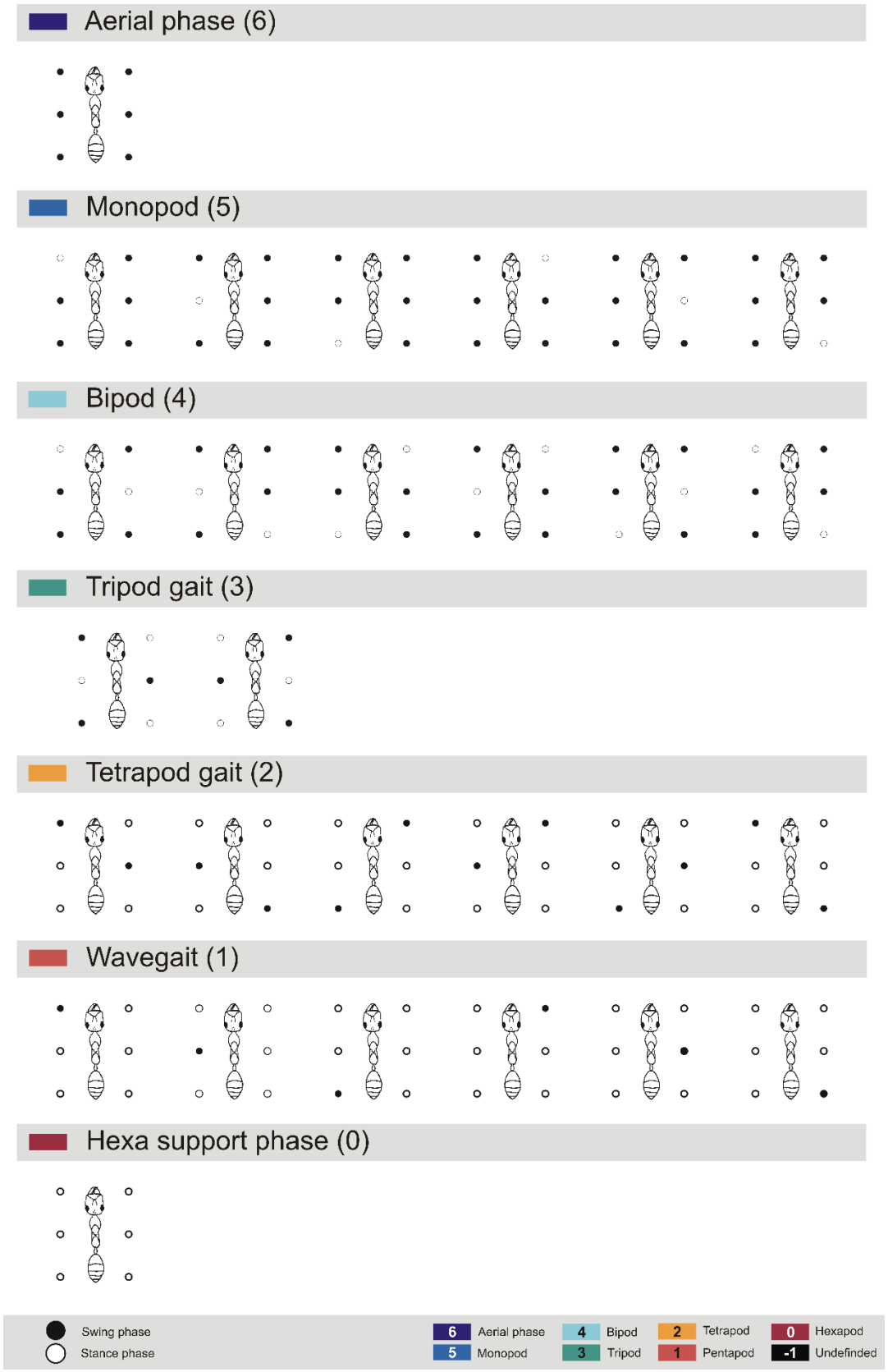

Figure S3 | Gait Patterns. According to the combination of legs in stance and swing phase (white and black dots, respectively), a video frame was assigned a certain leg coordination pattern (marked by colour or number). If none of the combinations depicted above was applicable, the frame was assigned category 'undefined' (black, -1). Note that these walking patterns are not defined by the mere number of legs in swing or stance phase, but are defined by a certain combination of specific legs in swing or in stance phase.

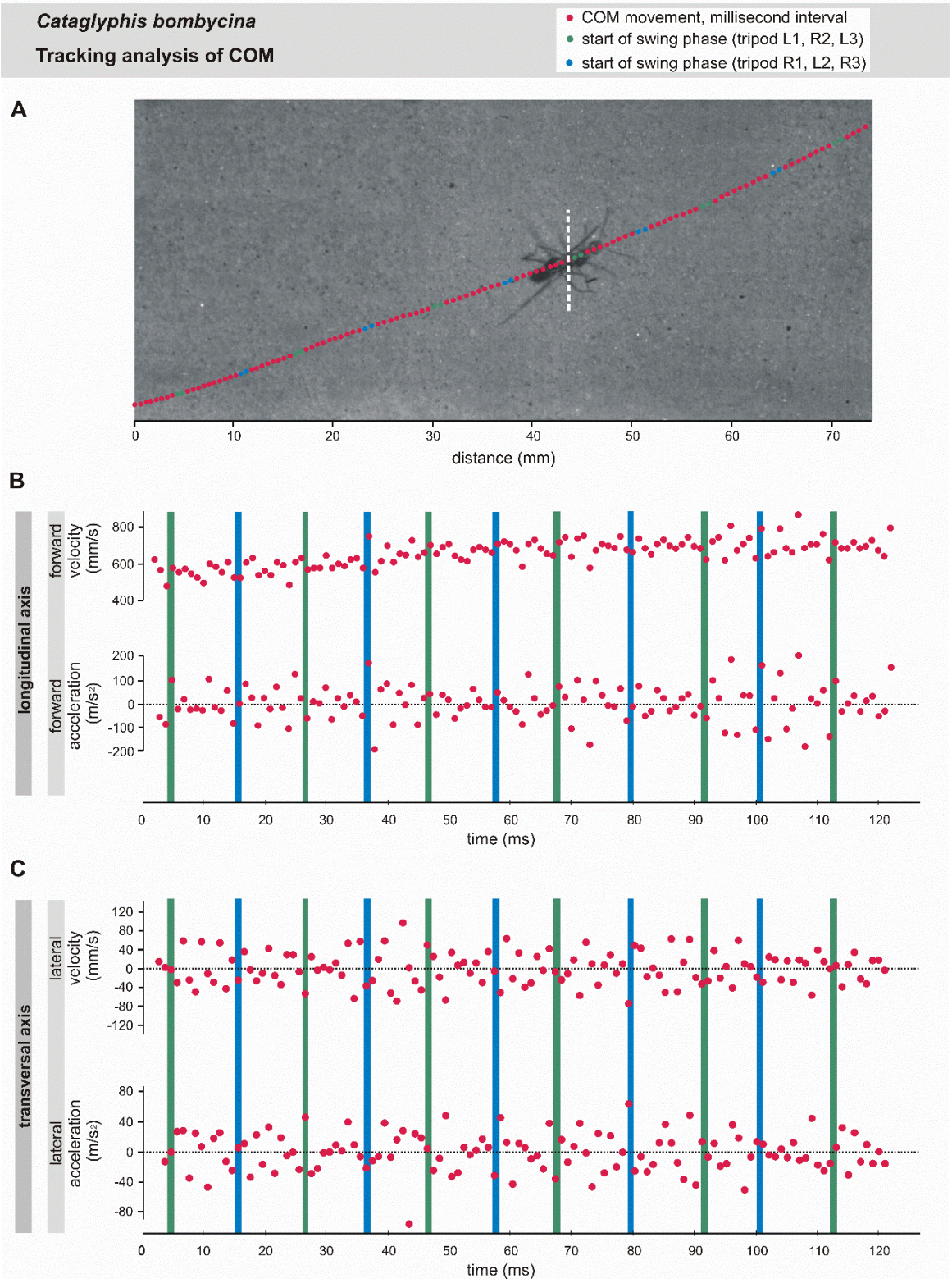

Figure S4 | Tracking of movement of the centre of mass (COM) in the horizontal plane during fast walking (653 mm/s) in *C. bombycina*. (**A**) The petiole was taken as proxy for the COM (Reinhardt and Blickhan, 2014) and tracked frame by frame for a given video recording. The top view provided in our video recordings allowed analysis of movement only in the horizontal plane. Each data point represents the petiole position in a 1 ms video frame (white dashed line marks petiole position in the depicted video frame); green data points indicate start of swing phase in one tripod (L1, R2, L3), blue data points start of swing in the other tripod (R1, L2, R3). **(B)** Forward velocity

and acceleration (along the longitudinal axis), (**C**) lateral velocity and acceleration of petiole movement (i.e. in the transversal axis), calculated from the sample recording in (A).

Walking dynamics and stability during insect locomotion can be described by sagittal and horizontal spring-mass-models, where rhythmic oscillations of COM are considered (Blickan and Full 1993, Schmitt et al. 2002**, Weihmann 2013***). We thus analysed speed and acceleration of fast-moving desert ants to assess the applicability of this model to the desert ant locomotion, with regard to horizontal movements. However, note that there is no apparent variation in speed or acceleration in the rhythm of the step cycle, neither for longitudinal nor for transversal movement of COM. Here, COM movement is dominated by straight translational movement in the posterior-anterior direction (average forward displacements during 1 ms interval is 0.65 mm in *C. bombycina*). Transversal fluctuations of the COM are minimal and appear to be dominated by measurement noise (lateral distance of COM to straight regression line on average 0.015 mm in *C. bombycina*).

** **Schmitt, J., Garcia, M., Razo, R. C., Holmes, P., and Full, R. J.** (2002). Dynamics and stability of legged locomotion in the horizontal plane: a test case using insects. *Biological cybernetics* **86**, 343-353.

*** **Weihmann, T**. (2013). Crawling at high speeds: steady level locomotion in the spider *Cupiennius salei* — global kinematics and implications for centre of mass dynamics. *PLoS One*, **8**, e65788.

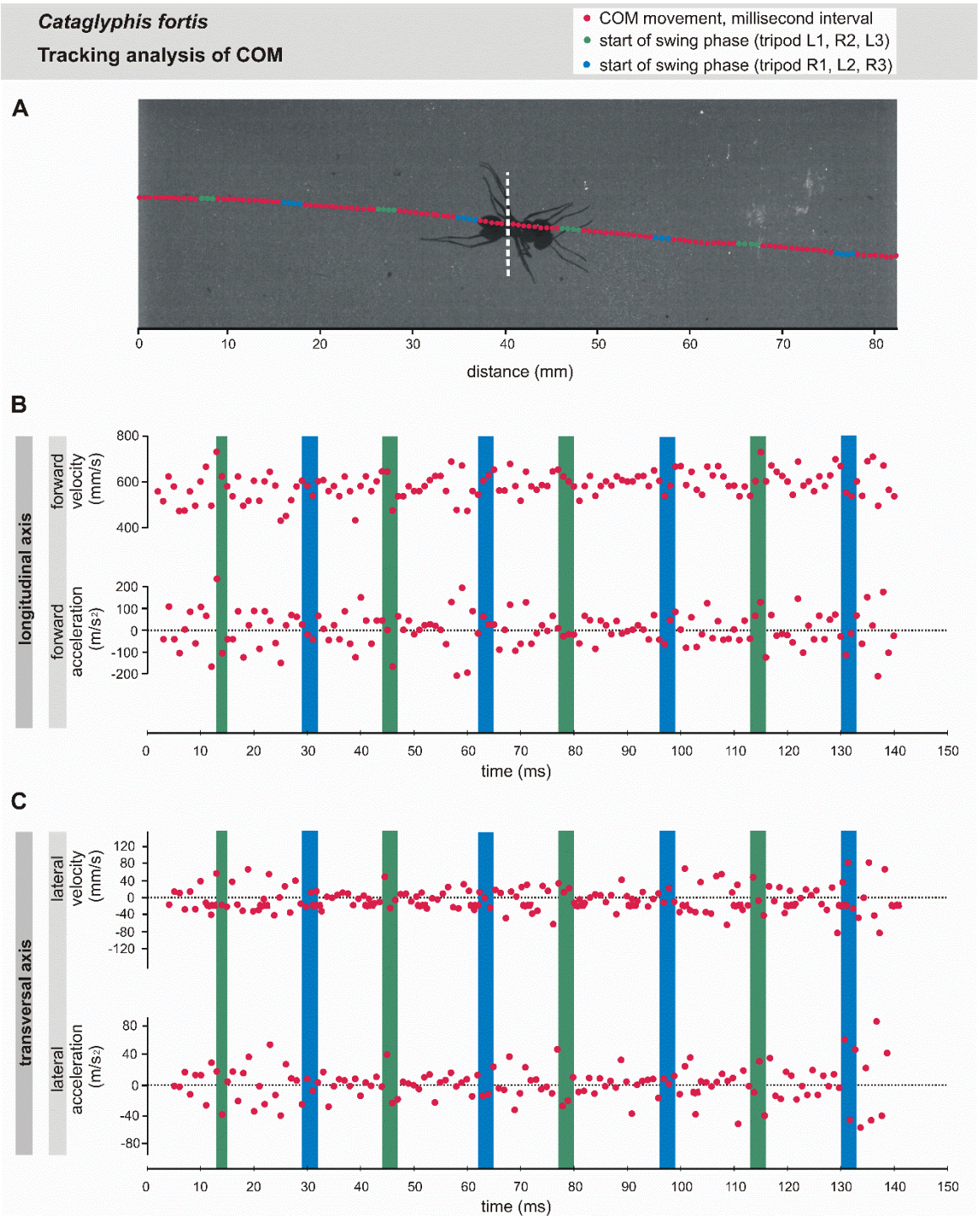

Figure S5 | Tracking of movement of the centre of mass (COM) in the horizontal plane during fast walking (591 mm/s) in *C. fortis*. Presentation of data as in Fig. S4, (**A**) to (**C**). Average forward displacements during 1 ms interval in C. *fortis* is 0.58 mm, lateral distance of COM to straight regression line on average is 0.016 mm (compare figure legend of Fig. S4).